RESEARCH PAPER

RNA Biology 11:11, 1430–1446; November 2014; Published with license by Taylor & Francis Group, LLC

Splicing changes in SMA mouse motoneurons and SMN-depleted neuroblastoma cells: Evidence for involvement of splicing regulatory proteins

Qing Huo[1,2], Melis Kayikci[3], Philipp Odermatt[1,2], Kathrin Meyer[1,#], Olivia Michels[1], Smita Saxena[1,4], Jernej Ule[3,+], and Daniel Schümperli[1,*]

[1]Institute of Cell Biology; University of Bern; Bern, Switzerland; [2]Graduate School for Cellular and Biomedical Sciences; University of Bern; Bern, Switzerland; [3]MRC Laboratory of Molecular Biology; Cambridge, UK; [4]Friedrich Miescher Institute for Biomedical Research; Basel, Switzerland

Current affiliation: [#]Center for Gene Therapy; Nationwide Children's Hospital; Columbus, OH USA; [+]Department of Molecular Neuroscience; UCL Institute of Neurology; London, UK

Keywords: exon junction microarray, laser capture microdissection, major spliceosome, minor spliceosome, motoneurons, neurodegerative disease, snRNP assembly, Spinal Muscular Atrophy, splicing, splicing regulators

Abbreviations: ESE, exonic splicing enhancer; FCS, fetal calf serum; hz, heterozygote, LCM; laser capture microdissection; MN, motoneuron; NMD, nonsense-mediated mRNA decay; NMJ, neuromuscular junction, PCR; polymerase chain reaction, qPCR; real-time (quantitative) PCR; RT, reverse transcription; sh, short hairpin; SMA, Spinal Muscular Atrophy; SMN, Survival Motor Neuron; snRNP, small nuclear ribonucleoprotein; snRNA, small nuclear ribonucleic acid; TcRβ, T-cell receptor β chain.

Spinal Muscular Atrophy (SMA) is caused by deletions or mutations in the Survival Motor Neuron 1 (*SMN1*) gene. The second gene copy, *SMN2*, produces some, but not enough, functional SMN protein. SMN is essential to assemble small nuclear ribonucleoproteins (snRNPs) that form the spliceosome. However, it is not clear whether SMA is caused by defects in this function that could lead to splicing changes in all tissues, or by the impairment of an additional, less well characterized, but motoneuron-specific SMN function. We addressed the first possibility by exon junction microarray analysis of motoneurons (MNs) isolated by laser capture microdissection from a severe SMA mouse model. This revealed changes in multiple U2-dependent splicing events. Moreover, splicing appeared to be more strongly affected in MNs than in other cells. By testing mutiple genes in a model of progressive SMN depletion in NB2a neuroblastoma cells, we obtained evidence that U2-dependent splicing changes occur earlier than U12-dependent ones. As several of these changes affect genes coding for splicing regulators, this may acerbate the splicing response induced by low SMN levels and induce secondary waves of splicing alterations.

Introduction

Spinal Muscular Atrophy (SMA) is a hereditary disease that leads to degeneration of motoneurons (MNs) in the spinal cord and consequently to muscle atrophy. Its occurrence rate and carrier frequency have been estimated at ~1/10'000 and ~1/50, respectively, with some differences due to ethnic origin.[1-4] SMA is considered rare, but it is nevertheless the most frequent inherited disorder leading to death in infants.

The disease-causing gene Survival Motor Neuron (*SMN*) is duplicated on human chromosome 5.[5] In SMA patients, a complete loss of function of *SMN1* is responsible for ~95% of cases, but at least one copy of *SMN2* remains. A crucial difference between *SMN1* and *SMN2* is the nucleotide at position 6 of exon 7: a cytosine in *SMN1* is part of a SRSF1-dependent exonic splicing enhancer (ESE) that favors exon 7 inclusion; in contrast, a thymidine in *SMN2* interrupts this ESE and creates an hnRNPA1-dependent splicing silencer resulting in predominant exon 7 skipping.[6-10] As a consequence, SMA is due to low levels of full-length, functional SMN protein.

The SMN protein has one well-established function and several additional proposed ones. Its biochemically best characterized function is to mediate, in complex with several other proteins called Gemins, the assembly of small nuclear ribonucleoproteins (snRNPs) involved in splicing and other RNA processing reactions (reviewed in[11]). The snRNPs which get assembled by the SMN complex are the major spliceosome components U1, U2, and U4, the minor spliceosomal snRNPs U11,

*Correspondence to: Daniel Schümperli; Email: daniel.schuemperli@izb.unibe.ch
Submitted: 06/13/2014; Revised: 10/16/2014; Accepted: 11/05/2014
http://dx.doi.org/10.1080/15476286.2014.996494

U12 and U4atac, the U5 snRNP common to both types of spliceosomes, and the U7 snRNP involved in 3' end processing of histone mRNAs. Whether SMN also plays a role in the assembly of the Lsm protein-containing snRNPs U6 and U6atac has not been established. Because the SMN-dependent snRNP assembly is essential to maintain splicing in all cells, it is not immediately evident how reduced SMN levels could lead to a MN-specific disease through this function.[12,13] However, SMN levels might be more limiting in MNs than other cells, either because the missplicing of *SMN2* may be more pronounced[14] or because of a higher demand for snRNPs. Another possibility is that the missplicing ensuing from reduced snRNP assembly may be exclusively detrimental for MNs, because the products of certain genes misexpressed in these cells happen to be essential for MN function and survival. Variants of this hypothesis propose that SMN may act in minor tri-snRNP assembly[15] or intranuclear snRNP mobility[16] and that alterations in these functions may cause splicing defects. In support of this snRNP-centered hypothesis for SMA pathogenesis, the snRNP assembly activity of SMN point mutations has been found to correlate with disease severity in transgenic mouse models.[17,18] Moreover, Fischer and co-workers working with zebrafish embryos have been able to counteract MN growth defects induced by antisense oligonucleotide-mediated SMN depletion by injecting snRNPs isolated from HeLa cells.[19]

Regarding additional, possibly MN-specific functions, there are indications that SMN might be involved in the assembly of other ribonucleoprotein particles such as snoRNPs,[20] telomerase,[21] or the signal recognition particle.[22] Moreover, in cultured neuronal cells, SMN has been localized in axonal outgrowths together with other factors of RNA metabolism such as Gemins 2 and 3, hnRNP Q and R, HuD, or FMRP, suggesting that it might play a role in axonal mRNA transport (reviewed in[13]). SMN-containing granules have been described to be associated with the COP1 complex involved in vesicular transport[23] and with the Golgi network.[24] Furthermore, SMN has been proposed to have an anti-apoptotic role in neurons,[25-28] and to be involved in transcription regulation[29] or neuronal migration and differentiation.[30-32] In *Drosophila*, SMN has also been suggested to play a role in stem cell division, proliferation and differentiation.[33]

On a cellular and organismal level, it is interesting to note that the first SMA symptoms, at least in mouse SMA models, do not appear to affect the MN cell bodies, but rather the periphery, i.e. the neuromuscular junctions (NMJ).[34-36] NMJ abnormalities have also been demonstrated in several muscles of 14 week-old human fetuses with SMA type I.[37]

The role of snRNP assembly defects in SMA has been mostly addressed by measuring snRNA levels and by assessing global mRNA splicing. Two studies showed that a reduction of SMN leads to an imbalance of snRNPs; in particular snRNPs of the minor (U12-dependent) spliceosome seemed to be affected.[35,36] In one microarray study carried out with whole spinal cord of advanced stage SMA mice, massive splicing changes were observed,[38] but other microarray studies in presymptomatic mice[39,40] or in a mild SMA model[41] failed to reveal widespread splicing changes. One particular U12-dependent splicing event has recently been highlighted as a possible cause contributing to SMA pathology: missplicing of a U12 intron in the gene *Tmem41b* (known as *Stasimon* in *Drosophila*) leads to a reduction of the Tmem41b protein which seems to be important for maintaining motor circuit function.[42]

Based on the above, we considered it worth to carry out another analysis of SMA-induced splicing defects because of certain novel features that we designed into our project. In particular, we isolated MNs by laser capture microdissection (LCM) which means that our samples were highly enriched in the cells relevant for SMA. Apart from a recent study which was published while we were writing this manuscript,[43] our study is so far the only large-scale analysis carried out with LCM-isolated MNs from SMA mice. As another modification compared to previous studies, we have used exon junction microarrays that allow for a very detailed analysis of alternative splicing events. Finally, we had the unique possibility to compare not only healthy mice and SMA mice, but also SMA/U7 mice in which the disease is prevented or partly corrected.[44]

This analysis revealed a considerable number of strong changes in U2-dependent splicing events. By comparison with other global splicing studies carried out with whole spinal cord RNAs, our results suggest that splicing alterations may be more abundant and occur earlier in MNs than in other parts of the spinal cord. Changes in U12-dependent splicing events were not detected by the microarrays, but some could be identified by RT-PCR analysis of LCM-isolated MN RNA. However, in a model of progressive SMN depletion in NB2a neuroblastoma cells, changes in U2-dependent splicing seemed to occur earlier and affect more genes than alterations in U12-dependent splicing. Furthermore, strong reductions of multiple U snRNAs occurred only after prolonged SMN depletion in this model, and snRNAs of the minor spliceosome did not appear to be preferentially reduced. Importantly, we also found multiple genes encoding splicing regulators and modifiers of such regulators to be affected at the splicing level. This suggests that low levels of SMN can trigger a cascade of splicing alterations in which the affected splicing regulators alter the splicing of an ever growing number of genes.

Results

Microarray analysis reveals splicing changes in motoneurons from the severe SMA mouse model

To study splicing defects in SMA, we analyzed RNA from MNs of lumbar spinal cord segments of 3–4 day-old mice (postnatal day 3, P3) of the severe SMA mouse model.[45] In this model, 2 allelic copies of human *SMN2* allow survival of mouse *Smn* knock-out animals until 5–7 d after birth. At 3–4 days, the numbers and morphologic appearance of MNs are still normal. First pathological signs can be seen in NMJs of the diaphragm and intercostal muscles that are innervated by the cervical and thoracic segments of the spinal cord, respectively.[46,47] However, calf muscles which are innervated from lumbar segments appear normal. It has not been thoroughly investigated whether more proximal hindlimb muscles or muscles from the lower trunk that also get innervated from lumbar spinal cord segments may show some pathology in this model and at this age. Whichever is the case, our

samples can be said to represent an early, but symptomatic stage of the disease.

More specifically, MNs were isolated by LCM from lumbar spinal cord sections of 4 animals each of the following genotypes: *mSmn* +/−, *hSMN2* +/+ (heterozygote/hz); *mSmn* −/−, *hSMN2* +/+ (SMA mice); and *mSmn* −/−, *hSMN2* +/+ carrying several copies of a therapeutic U7 gene known to correct the SMA phenotype (SMA/U7 mice;[44]). RNA isolated from these MNs was amplified and reverse transcribed, and the cDNAs were hybridized to Affymetrix exon junction arrays.

For the evaluation, the samples were subjected to 4 pairwise comparisons (**Fig. 1A**). The first 3 SMA mice were compared to the first 3 hz mice as well as to the first 3 SMA/U7 mice. Similarly, the SMA mice 2–4 were compared to the mice 2–4 of the other 2 groups. The reason for this procedure was that the ASPIRE software[48] used for the analysis allowed for only 3 arrays in each pair to be compared. This gave us 2 separate values for each comparison, even though these were not completely independent, because 2 of the mice from each group were shared.

The values initially analyzed were dI (the change in% inclusion of the particular probe) and dIrank (a statistical ranking of the splicing change). According to the experience of the Ule lab and members of the EURASNET consortium who worked with these arrays previously, dIrank values >1 or <−1 should give a RT-PCR validation rate of ~85% when tested in the same biological system.[48] We then calculated mean values for these 2 parameters from the 4 pairwise comparisons described above. To facilitate the ranking and grouping of these values, we additionally gave positive and negative score points if the mean dI of a comparison was equal or larger than 25% in positive or negative direction, or if the mean dIrank was ≥ 0.75 or ≤ −0.75. Thus, any given probe could reach a sumscore value of maximally plus or minus 8 points from all 4 comparisons.

Of the 32′875 probes present on the microarrays, 27′729 were informative.

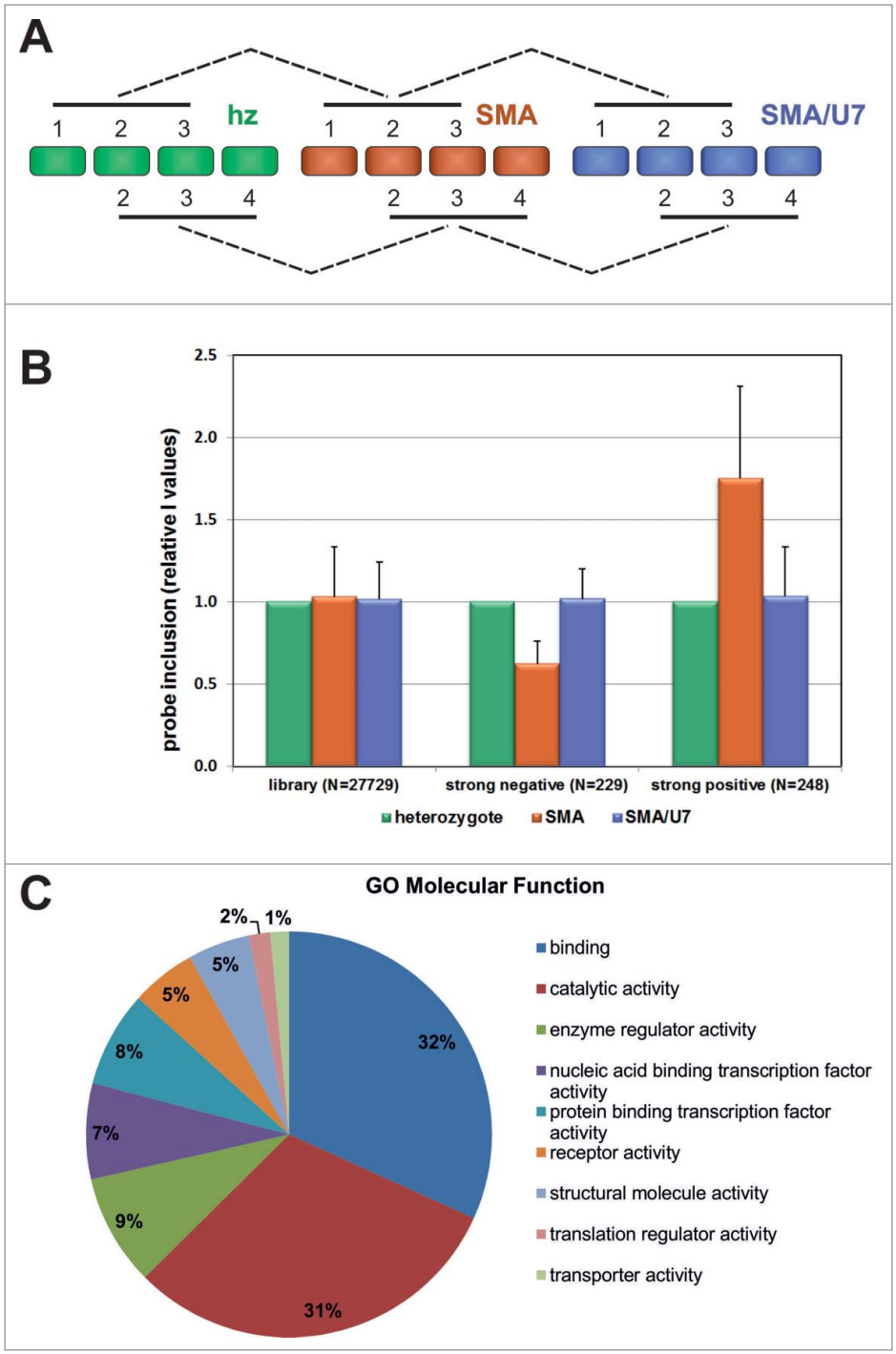

Figure 1. Summary of microarray data. (**A**) Schematic representation of microarray comparisons. SMA mice 1–3 were compared to heterozygous (hz) mice 1–3 and to SMA/U7 mice 1–3. Similarly, SMA mice 2–4 were compared to the mice 2–4 of the other 2 groups. In SMA/U7 mice, *SMN2* mRNA splicing and the SMA phenotype are partly corrected by the expression of a therapeutic U7 snRNA trans--gene[44]. (**B**) Summary of relative probe inclusion (I) values in hz and SMA mice as well as in SMA/U7 mice. Error bars represent standard deviations. P values for 2-sided Student T test: strongly excluded (N = 229), SMA vs. hz, 2.2 x 10^{-154}, SMA vs. SMA/U7, 1.6 x 10^{-90}, SMA/U7 vs. hz, 0.068; strongly included (N = 248), SMA vs. hz, 3.4 x 10^{-70}, SMA vs. SMA/U7, 2.2 x 10^{-54}, SMA/U7 vs. hz, 0.077. (**C**) Gene ontology analysis of molecular functions (performed at www.pantherdb.org) of genes showing strong splicing changes (see Tab3 of Supplementary File 1 for analyses of further categories).

Table 1. Statistics of microarray data

		dI			dI rank			sumscore		
	number	mean	max	min	mean	max	min	mean	max	min
total probes	32875									
informative probes	27729	0.162			0.005					
negative strong	229	-26.895	-66.125	-10.785	-1.165	-4.063	-0.750	-4.594	-8	-3
positive strong	248	27.209	56.805	11.030	1.235	6.770	0.750	4.810	8	3

dI: difference in % probe inclusion of SMA mice compared to heterozygous and SMA/U7 mice
dI rank: statistical ranking of splicing changes; dIrank values >1 or <-1 should give a RT-PCR validation rate of of $\sim$85%[48]
sumscore: score points were given when the absolute dI value of a comparison was $\geq$ 25% or when the absolute dIrank was $\geq$ 0.75; as each probe was compared twice between SMA and wt and twice between SMA and SMA/U7, and the score points given had positive or negative values depending on the direction of the splicing change, any given probe could reach a sumscore value between $+8$ and -8 points from all four comparisons.

Probes with absolute sumscore values $\geq$3 and absolute average dIrank $\geq$0.75 were placed in groups of strong positive and strong negative splicing changes. From these initial groups, we manually eliminated some probes with small differences between SMA and wt animals or with contradictory results. This resulted in 229 and 248 probes with strongly positive or negative splicing changes, respectively (**Table 1**). The vast majority (82%) were predicted to be more strongly included or skipped cassette exons. The remaining events were equally distributed among alternative 5′ or 3′ exons and intron retention events. All changes affected major, U2-dependent exons. Full lists of these strong positive and strong negative events are presented in Tabs 1 and 2, respectively, of the Supplementary File 1. A statistical comparison of the mean dI values of these 2 groups to the entire library is shown in **Figure 1B**. The relatively high standard deviations reflect the fact that the mean dI values cover a broad range between about 60 and 10% probe inclusion or exclusion (**Table 1**). Importantly, however, the average dI values of SMA animals in both groups differ very significantly from those of the healthy heterozygous (hz) or U7/SMA mice. In contrast the values of the SMA/U7 and hz mice show no significant difference. This indicates that the splicing changes detected by the microarray are indeed caused by the SMA genotype and do not occur or are strongly reduced in SMA/U7 mice. In contrast, averaged over the entire set of 27'729 informative probes, there was almost no change between the different mouse genotypes (Average dI and dIrank of 0.162 and 0.005, respectively).

We then performed a gene ontology analysis at the PANTHER website (www.pantherdb.org) for the entire set of genes showing strong splicing changes. Of 353 genes that were properly identified by the software, $\sim$70% of 406 hits fell into the following 3 molcular function categories: binding (31.8%, mostly nucleic acid-binding), catalytic activity (30.8%) and transcription factor activity (8.9%) (**Fig. 1C**). The three most prominent identified biological processes (total number of hits: 607) were: metabolic (29.5%, mostly nucleobase and protein metabolism), cellular (21.3%, mostly cell communication and cell cycle) and localization (9.9%, mostly vesicle-mediated and protein transport) (see Tab 3 of the Supplementary File 1 for further details).

Finally, the microarray analysis also revealed expression changes of certain RNAs (see Tabs 4 and 5 of Supplementary File 1), but many of these transcripts were not annotated, and the splicing alterations appeared more prevalent.

Candidate validations in SMA mouse motoneurons and SMN-depleted NB2a neuroblastoma cells

We then proceeded to validate some of the splicing changes revealed by the microarray analysis. Initially, we tried to do this by performing RT-PCR of whole spinal cord RNA from SMA and hz mice at P3. However, none of the genes tested by this approach showed any splicing changes (for an example see **Fig. 3** below). The failure to detect splicing differences by this approach may have been due to the fact that MNs represent only a small fraction of all spinal cord cells. Thus changes in MNs may have been masked by a constant or inverse splicing behavior in the other cells. To circumvent this problem, we then used RNA isolated from microdissected lumbar spinal cord MNs (i.e., identical material as used for the microarrays). However, because of the methodological difficulty and the low yield of material, we were able to validate only a few selected events by this method.

As a third strategy, we used RNA from NB2a mouse neuroblastoma cells that were partly depleted of SMN by transient RNA interference. This cell culture model allowed us to analyze more splicing events and to obtain a larger picture of the order of events (see below). In this model, the level of mouse SMN mRNA was reduced to $\sim$15% after 3 d and to $\sim$5% after 5 d of SMN depletion, and the SMN protein was similarly reduced, to 14% and 9%, respectively (**Fig. 2**). Thus the depletion was progressive over this time period but somewhat less extensive than in P3 severe SMA mice, where SMN transcripts were barely detectable by conventional RT-PCR (see **Fig. 3** below). As a comparison for protein levels, we previously found SMN protein levels in spinal cords of P3 severe SMA mice to be less than 10% of wild-type levels.[44] Usually, the NB2a cells were still proliferating until 3 d post-transfection, albeit at a reduced rate compared with control cells depleted of T cell receptor β (TcRβ). At this time point, proliferation ceased and cells started to die so that cell numbers were usually reduced 2- to 4-fold by 5 d (data not shown). Based on metabolic measurements (resazurin assays), the metabolic activity of cells at 3 d of MN depletion was reduced to $\sim$60% of control cells, while residual cells at 5 d of depletion showed only $\sim$35% metabolic activity (**Fig. S1** of Supplementary File 2).

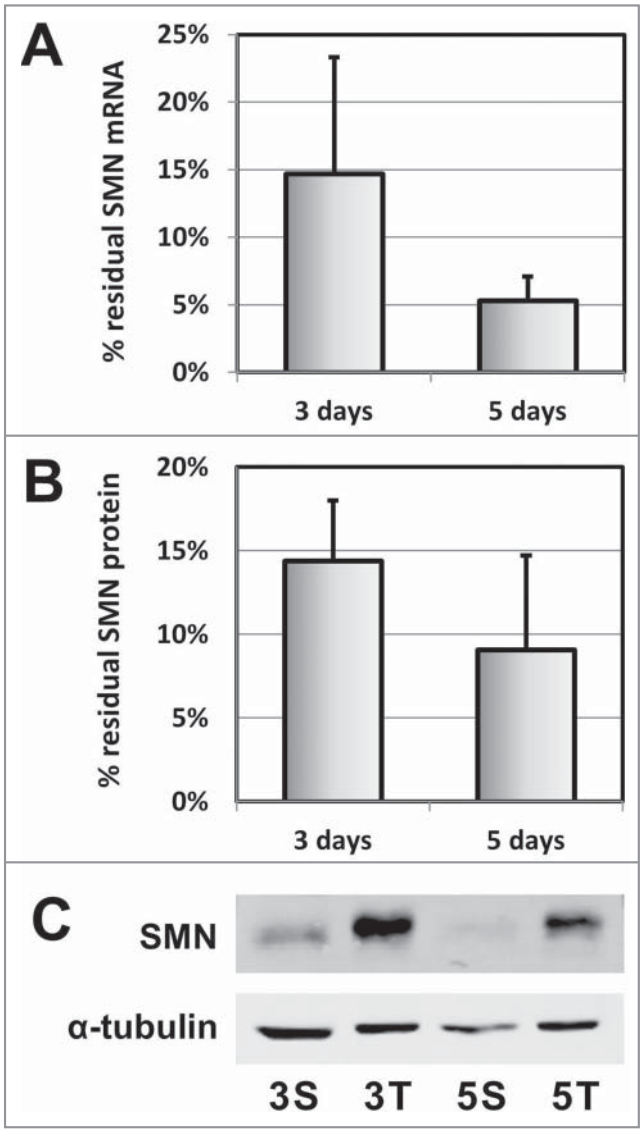

Figure 2. Quantitation of residual SMN expression in SMN-depleted NB2a cells. Mouse NB2a neuroblastoma cells were depleted of SMN for 3 or 5 d (designed below as 3S and 5S, respectively). As control, the cells were similarly depleted of TCRβ which should not be expressed in these cells (3T and 5T). (**A**) Transcript levels were analyzed by RT-qPCR using 5.8S rRNA as a reference. Error bars represent standard deviations. P values for 2-sided Student T test (N = 8): 3S vs. 3T, 1.1×10^{-13}, 5S vs. 5T, 8.4×10^{-20}, 3S vs. 5S, 0.013. **(B, C)** For the analysis of protein levels, whole cell extracts were analyzed by Western blotting with antibodies detecting mouse SMN and α-tubulin. Images were analyzed and bands quantitated as described in Materials and Methods. A representative Western blot is shown in C, and the compiled results of 6 experiments are summarised in B. P values for 2-sided Student T test: 3S vs. 3T, 5.6×10^{-14}, 5S vs. 5T, 2.6×10^{-12}, 3S vs. 5S, 0.081.

In the NB2a cell model, we analyzed 92 candidates from the list of strongly altered splicing events identified in the MN microarray analysis. We preferentially chose strongly altered events as predicted by the microarrays or events in genes considered to be important for gene regulation or the development and functions of the nervous system. When the cells had been depleted of SMN for 3 days, 16 of these events showed strong changes and 6 showed mild alterations, amounting to ~24% of all analyzed events (Tables 2a and 2b). The other events either yielded unclear results, showed no change, or the transcripts were not detectable in NB2a cells. Interestingly, 9 of the 22 affected events changed in the opposite direction from the one predicted by the microarrays. Nevertheless, the majority of changes (13) was in the same direction as indicated by the microarrays.

Moreover, 17 splicing events were analyzed with RNA samples from microdissected MNs. As the laser capture microdissection was very labor-intensive and yielded only small amounts of RNA, we restricted this type of assay to genes for which we had previously detected splicing changes in NB2a cells or to events that were ranked as most highly altered in the microarray results. Among these, we could detect changes in 7 splicing events (Tables 2a and 2b). For six of these, the splicing change was as predicted by the microarrays. Only for one gene (*A2bp1/Rbfox*, see below), the change was in the opposite direction compared to the microarray results.

Examples of these analyses are shown in **Figure 3**. The transcription factor E2F6 may play a role in the silencing of target genes and in controlling the cell cycle.[49] The microarray indicated an increased use of a 66 nucleotide exon (termed here 1a) that leads to truncation of the open reading frame due to an in-frame stop codon. In isolated MNs, only the upper band corresponding to the inclusion of the additional exon could be detected by RT-PCR, and its amounts seemed to be increased in SMA mice (**Fig. 3**, first row). The splicing of *E2f6* was also analyzed in RNAs from whole spinal cord and heart. In these samples, both products were detected, but their ratio did not change. As previously mentioned, also other genes, when tested in whole spinal cord RNA, did not show any of the changes indicated by the MN microarrays. However, in NB2a cells depleted of SMN, *E2f6* showed the increased use of the alternative exon predicted by the microarrays.

Aftiphilin (*Aftph*) is a component of the clathrin machinery in neurons that co-localizes at synapses with synaptophysin and with the AP-1/AP-2 clathrin adaptor complexes.[50,51] In agreement with our microarray data, the use of exon 8 (81 nucleotides, open reading frame retained) could be shown by RT-PCR to increase in MNs of SMA mice (**Fig. 3**, second row). However *Aftph* is one of several genes that showed an inverse splicing change in NB2a cells compared to MNs. The effects of these changes on the protein are unknown, as no functional domains have been characterized.

The third example is the gene encoding the protein "RGD motif, leucine rich repeats, tropomodulin domain and proline-rich containing" (*Rltpr*) also known as "Leucine-rich repeat protein 16c" (*Lrrrc16c*). This gene produces a transcript of 37 exons encoding leucine-rich repeats in the N-terminal half, a motif interacting with the actin filament capping protein and a C-terminal proline-rich region. The protein and its different paralogs may be involved in actin filament uncapping.[52-54] Moreover Rltpr was recently shown to play a role in CD28 co-stimulation of T-cells.[55] The alternative exon (termed here 35a) adds 27 amino acids to the proline-rich region. The use of this exon was

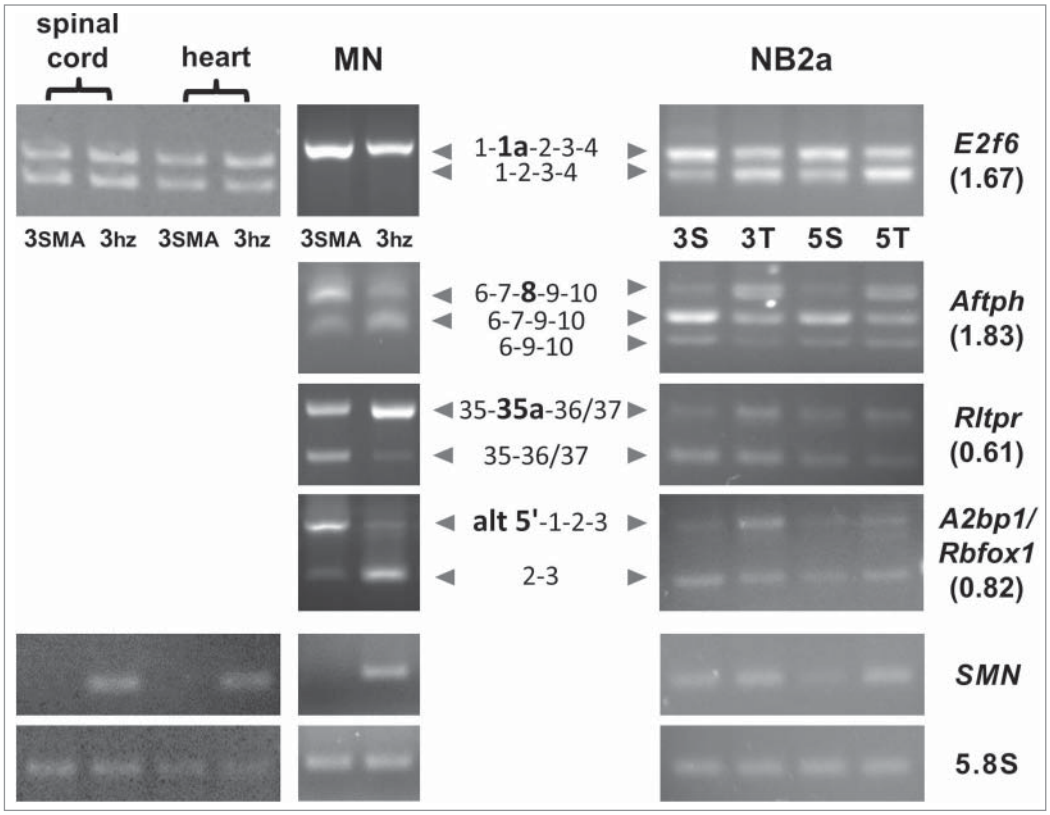

Figure 3. Validation of splicing changes by RT-PCR. Analyses shown on the left were performed with cDNA from spinal cord, heart and LCM-isolated motoneurons (MN) prepared from P3 SMA (3SMA) and heterozygous mice (3 hz). Panels on the right show analyses of cDNA from mouse NB2a neuroblastoma cells that had been depleted of SMN for 3 or 5 d (lanes labeled 3S and 5S, respectively). As control, the cells were similarly depleted of TCRβ which should not be expressed in these cells (3T and 5T). The splicing of the gene region of interest was analyzed by RT-PCR with appropriate primers. Gene symbols are listed on the right; numbers in brackets represent the fold change in probe inclusion (dI) as calculated from the microarray data (1 = equal inclusion). The central column indicates the exons contained in the various amplicons; exons of interest are shown in bold and larger font size; alt 5′: alternative 5′ exon; a: alternative exon. The lower sections show RT-PCR products of endogenous mouse *SMN* RNA to illustrate the extent of depletion and of 5.8S rRNA used as loading control.

reduced in MNs from SMA mice as predicted by the microarrays as well as in SMN-depleted NB2a cells (**Fig. 3**, third row).

Finally, we show the results obtained for *A2bp1/Rbfox1*. This "Fox1 homolog A," also known as "ataxin 2-binding protein 1" or "hexaribonucleotide-binding protein 1" contains an RNA recognition motif[56] and may thus be involved in neuronal splicing regulation, similar to Fox1. However it also binds to the C-terminus of ataxin-2 and co-localizes with ataxin-2 in the trans-Golgi network.[56] The microarrays had indicated a reduced use of an alternative 5' exon in SMA mice which could also be detected in SMN-depleted NB2a cells (**Fig.3**, fourth row). However, *A2bp1/Rbfox1* is the only gene for which we observed an inverse splicing change between RT-PCR and microarrays of isolated MN RNA.

Some, but not all, of these splicing changes became more prominent as the SMN depletion progressed to 5 d As examples for this type of behavior, RT-PCR analyses of *Ewsr1* and *Deaf1* are shown in **Figure 4** (1st and 2nd row). Both of these gene products are thought to be involved in the regulation of transcription or RNA metabolism (**Table 2a**). Moreover, additional splicing events began to be affected with longer, more extensive SMN depletion, such as the switch between 2 alternative 5' exons in *Sept9* (**Fig. 4**, 3rd row). Sept9 is a member of the septin family involved in cytokinesis and cell cycle control,[57] and certain mutations in this gene can cause the disease Hereditary Neuralgic Amyotrophy.[58]

Changes in U12-dependent splicing become apparent after prolonged/extensive SMN depletion

Interestingly, there were no U12-dependent events among the top-listed splicing changes of our MN microarray data. This finding was unexpected, because reductions in minor U snRNAs[17,38,42] and splicing alterations in U12-introns[42] had been described as one of the hallmarks of SMA. Two reasons might be responsible for this apparent lack of U12-dependent splicing changes: first, U12-dependent splicing events may be underrepresented in the microarrays; secondly, the usual outcome of an impaired U12-dependent splicing event should be the retention of the U12-intron; this may easily escape detection, because intron-containing RNAs can be degraded rapidly, e.g. through the mechanism of nonsense-mediated mRNA decay (NMD).

Thus, we decided to analyze whether U12-introns do show alterations in our NB2a SMN depletion model and whether these alterations occur earlier or later than the changes seen in U2-dependent events. For this analysis, we tested a certain number of genes that had shown strong splicing changes in the microarrays but which contained U12-introns elsewhere in the gene. Additionally, we analyzed the splicing of the U12-introns present in *Tmem41B* and *Zpr1*, since the U12-intron of *Tmem41b* had been indicated as a potential pathogenic factor for SMA,[42] and Zpr1 (also known as Znf259) had been suggested to modify SMA.[59]

Interestingly, of 12 U12-dependent events that were detectable in NB2a cells, none showed changes at 3 d of SMN depletion by conventional agarose gel analysis of RT-PCR products. Only when the SMN depletion was prolonged to 5 days, we could detect an increased retention of the U12-introns of *Eed*

Table 2a. Summary of splicing changes (events with positive splicing change predicted by the microarray analysis).

Gene	sum-score	avg dI	avg dirk	region of interest	protein effect	MN	spinal cord	NB2a	full name	function
Lsamp	8	56.8050	3.3000	tr004 E3-E5	alt C-term	no change	no change	unclear[1]	Limbic system-associated membrane protein	homophilic adhesion molecule, neuronal growth and connections
Clk3	8	44.7050	1.3100	tr201 E4	97 nt, fs, loss of kinase domain, NMD?	n.a.	n.a.	*reduced*	CDC-like kinase 3	serine/threonine phosphorylation of SR proteins
Ank2	8	36.4550	1.6325	tr201 extd E11/ alt polyA > tr202	C-term truncation	**increased**	no change	*reduced*	Ankyrin 2	membrane to (actin-) cytoskeleton connection
Atp11c	7	28.9475	2.4450	tr001 E29	alt C-term	**increased**	no change	*reduced*	ATPase, class VI, type 11C	phospholipid transport, ER membrane
Aftph	7	27.5150	1.3850	tr201 E8	81 nt = 27 aa	**increased**	no change	*reduced*	Aftiphilin	neuronal clathrin machinery, synapses
Ewsr1	7	41.0375	0.9150	alt E5a/alt polyA, tr002 > tr010	C-term truncation	unclear[1]	n.a	**increased**	Ewing sarcoma breakpoint region 1	transcriptional activation/repression, RNA binding
E2F6	6	41.9625	1.1900	tr201 novel E1a	66 nt, PTC	**increased**[2]	no change	**increased**	E2F transcription factor 6	transcriptional repressor, cell cycle control
Deaf1	6	34.5825	1.0900	alt E2	AUG, alt N-term	n.a.	n.a.	*reduced*	Deformed epidermal autoregulatory factor 1	transcription, when secreted, regulator of cell proliferation
Scaf8/ Rbm16	6	25.7725	2.5700	5'ss in last exon spliced to novel downstream exon	alt 3' UTR	n.a.	n.a.	**increased**	SR-related CTD-associated factor 8	transcription, splicing
Mtf2	6	24.6350	1.3825	tr001 alt E10a	78 nt, fs, alt C-term, NMD?	n.a.	n.a.	**(increased)**	Metal response element binding transcription factor 2	regulator of chromatin
Ythdc1	4	19.8942	1.6025	tr001 E6	54 nt = 18 aa	no change	n.a	**increased**	YTH domain containing 1	Putative splicing factor or regulator
Igf1	3	17.0475	1.0767	tr003 E5	Ea > Ec form	contradict. results	n.a	*(reduced)*	Insulin-like growth factor 1	regulation of cell proliferation
Pkp4	3	13.6700	1.0250	tr001 E20	129 nt = 43 aa	n.a.	n.a.	*reduced*	Plakophilin 4	regulating junctional plaque organisation and cadherin function

Table 2b. Summary of splicing changes in Nb2A cells after 3 d SMN knockdown

Gene	sum-score	avg dI	avg dirk	region of interest	protein effect	MN	spinal cord	NB2a	full name	function
Taf2	-8	-53.0600	-1.6275	tr201 alt 3'ss E18	fs, NMD?	no change[1]	no change[1]	no change[1]	RNA polymerase II, TATA box binding protein (TBP)-associated factor 2	component of the general transcription factor TFIID and of TFTC-HAT complex
Rltpr	-8	-34.6525	-1.2175	tr203 E7 tr202 E35a	81 nt = 27 aa	**reduced**	n.a.	**reduced**	RGD motif, leucine rich repeats, tropomodulin domain and proline-rich containing	interacts with actin filament capping protein
Cstf2	-7	-39.5250	-1.1200	tr201 E9	60 nt = 20 aa	unclear	no change	**(reduced)**	Cleavage stimulation factor 64 kDa subunit	mRNA polyadenylation, poly(A) site selection
Sept9	-7	-30.7575	-0.8575	tr004 alt 5' E1	N-term truncation	n.a.	n.a.	**(reduced)**	Septin 9	cytoskeletal GTPase, cytokinesis
Snrpa1	-5	-21.1325	-1.2025	tr001 int6	IR, NMD?	no change[1]	n.a.	no change[1]	small nuclear ribonucleoprotein polypeptide A	U2 snRNP A' protein, splicing
Tia1	-4	-23.3050	-1.5350	tr001 E12 (& E11)	146 (& 124) nt = 90 aa	contradict. results	n.a.	*increased*	Cytotoxic granule-associated RNA-binding protein 1	RNA binding, ARE and TOP elements, apoptosis
Src	-4	-22.2200	-1.4350	tr201 E6	18 nt = 6 aa	unclear[1]	n.a.	**reduced**	Rous sarcoma oncogene	tyrosine-protein kinase, proto-oncogene
Plag1	-4	-14.6775	-1.2675	tr001 E5 & novel alt E4a (59 nt)	N-term truncation	not detectable	very low expression	**reduced**	Pleomorphic adenoma gene 1	transcription factor, IGF2 regulation
Pdcd2l	-3	-16.5150	-1.2725	tr001 E6	149 nt, alt C-term, fs	**reduced**	n.a.	*increased*	Programmed cell death 2-like	cell cycle and growth response
A2bp1/ Rbfox1	-3	-14.7225	-0.8375	alt 5' exon ~700 kb upstream of gene body	alt N-terminus	*increased*	n.a.	**reduced**	Ataxin-2 binding protein 1 / Fox1 homolog	RNA metabolism, splicing, transcript levels
Supt20h/ Fam48a	-3	-11.6075	-0.9575	alt 5' exon or alt 5'ss lengthening E1	5' UTR	n.a.	n.a.	**(reduced)**	Transcription factor SPT20 homolog	transcription, growth factor signalling
Pum1	-3	-10.7850	-0.8200	tr001 E14	237 nt = 79 aa	n.a.	n.a.	**(reduced)**	Pumilio 1 (Drosophila)	regulation of translation/stability of target mRNAs

For the genes/splicing events listed in Table 2a, the exons of interest showed increased use in the microarrays; those in Table 2b were used less. Sumscore, average dI and average dIrk are values derived from the microarray analysis. Experimentally determined splicing changes are listed for isolated motoneurons (MN), whole spinal cord and for NB2a cells after 3 days of SMN depletion. Events changing in the direction predicted by the microarrays are shown in bold letters and light grey shading, changes in the opposite direction are shown in italics. Experimentally derived splicing changes in NB2a cells that were arbitrarily considered weak are shown in brackets. n.a. and dark grey shading, not analysed; tr. . ., annotated transcript designation in EnsEMBL; E., exon number; alt, alternative; ss, splice site; int, intron; polyA, polyadenylation site; fs, frame shift; [1)] alternative transcript not detected; [2)] only alternative transcript detected, increased in MN samples.

and *Taf2* (**Fig. 5A**). For *Ap4m1* and *Tmem41b*, the levels of normal transcripts were reduced at 5 d (**Fig. 5B**) which may have been due to NMD triggered by aberrant splicing, as reported in the work of Lotti et al. 2012.[42] A marginal reduction of transcript levels was also seen for *Trit1* (data not shown). For the U12-introns in *E2f6* (**Fig. 5A**) and 6 other genes (*Eftud1*, *Mbtps2*, *Slc25a14*, *Tnpo2*, *Usp14*, *Zfp259*; data not shown), there was no clear indication of an intron retention, and the transcript levels appeared to remain unaffected.

The RT-PCR method used in the experiments described so far is useful to detect splicing changes, when 2 or more splicing products are produced and one finds changing ratios between these products. For a given sample, these ratios are robust over a wide range of RNA or cDNA input amounts and replication cycles (Ref.[60]; own unpublished results). However, when a single band is observed in varying quantities, this method is not reliable, as differences may disappear or be underestimated when the PCRs reach saturation. For this reason, the *Ap4m1* and *Tmem41b*) genes whose transcripts had shown reductions of a single band were reanalysed by quantitative (real-time) PCR of the cDNAs. This revealed that the level of *Ap4m1* mRNA was reduced to 54% of the level of the control cells after 3 d of SMN depletion and to 40% after 5 d (**Fig. 5C**). Similarly, the *Tmem41b* level was reduced to 72% after 3 d and to 40% after 5 d of SMN depletion. However, the change of this gene at 3 d was only slightly significant ($p = 0.041$).

These results indicate that changes in U12-dependent splicing events do occur in SMN-depleted NB2a cells but that they may require a prolonged and/or stronger SMN reduction to become detectable than U2-dependent events.

We then also tested the U12-exon containing *Ap4m1* and *Tmem41b* genes in LCM-isolated MNs of lumbar spinal cord. Indeed we could observe a similar reduction of transcript levels (**Fig. 5D**) as in the NB2a cells that had been depleted of SMN for 5 d (**Fig. 5C**).

We also tried to quantitate U snRNA levels by RT-qPCR in the SMN-depleted NB2a cells, in order to determine to what extent the observed splicing changes might be due to reductions in spliceosomal snRNP levels. However, as the results showed a relatively large degree of variation between experiments, it was difficult to draw strong conclusions. Nevertheless, these data indicated that strong reductions in multiple U snRNAs only become apparent after 5 d of SMN depletion, and that there is no obvious difference in the reduction between U snRNAs of the minor and major spliceosomes (**Fig. S2** of Supplementary File 2).

Discussion

SMA-induced splicing alterations appear to be more prevalent in motoneurons than in other neural tissues

This study was initiated to analyze one of the prevailing hypotheses for SMA pathogenesis. As SMN plays a central role in snRNP assembly,[11] this hypothesis proposes that an assembly defect could contribute to SMA pathogenesis in the sense that reduced snRNP levels may cause splicing changes, some of which may in turn affect vital functions in MNs.

Previous studies which addressed this point had analyzed splicing and transcript levels in whole spinal cord, sometimes in comparison with other tissues, from the severe[40] or $\Delta 7$[38-40] SMA mouse models and in one case also from a milder model.[41] The authors had used exon arrays which are somewhat less sensitive in detecting alternative splicing events than the exon junction microarrays used here. A consensus that could be derived from these studies was that wide-spread splicing defects are a feature of late symptomatic stages.[38-40] In contrast, no or only few changes were detected in pre-symptomatic or early symptomatic stages[39,40] or in the mildest analyzed SMA model.[41]

Our own study, as well as a recent paper[43] which used next generation sequencing for the analysis and that was published while we were writing our manuscript, are the first ones that have analyzed SMA-related splicing defects specifically in MNs. Together, they reveal a different picture regarding the prevalence of splicing changes in early phases of the disease. As discussed in the initial results section, our own samples from lumbar MNs of P3 mice can be regarded as early symptomatic. In the recent study by Zhang et al., the transcriptome of MNs was analyzed at a yet earlier stage.[43] These authors also isolated MNs from the lumbar region, but in P1 mice of the milder $\Delta 7$ model. As both studies revealed a considerable number of splicing changes, it appears that splicing may be affected in MNs more extensively and at an earlier time point than in other cells of the spinal cord. In agreement with this, we were not able to validate splicing changes in whole spinal cord, but could do so for several genes in cDNA from isolated MNs (**Fig. 3**). Similarly, Zhang et al. found fewer and different splicing changes in the white matter than in MNs of the same spinal cord sections.[43] This early affection of MN transcriptomes may be related to the finding that the skipping of *SMN2* exon 7 is also more pronounced in isolated MNs than in surrounding spinal cord tissue.[14]

When we compared our microarray data to those of the other, published studies,[38,39,43] we could identify 30 cases in which the same splicing event was changed or the change was at least likely to have affected the same exon(s) in 2 or more analyses (**Table 3**). Additionally, we found 14 matching genes for which we could not identify unambiguously which exon(s) were affected (**Table S1** of Supplementary File 2) and 18 cases where the same gene but different exons seemed to be affected (**Table S2** of Supplementary File 2). Note that, for the older exon array data, it is often difficult to determine exactly which splicing event is affected within a gene. For all but one of these studies, the certain or likely exact matches represent a small fraction (1–7%) of all identified splicing changes (**Table 3**). A further evaluation of the data from**Table 3** revealed that the matches fall into 2 main clusters (**Table 4**). One of these is represented by analyses of whole spinal cord samples of $\Delta 7$ mice at P7, P11 and P13 with a slightly less extensive overlap between P1 and P7 samples.[38,39] The second cluster consists of the 2 studies on isolated MNs from P3 mice of the severe model (our study) and $\Delta 7$ mice at P1.[43] This further underscores the notion that the transcriptomes of MNs are different from those of the remaining spinal cord

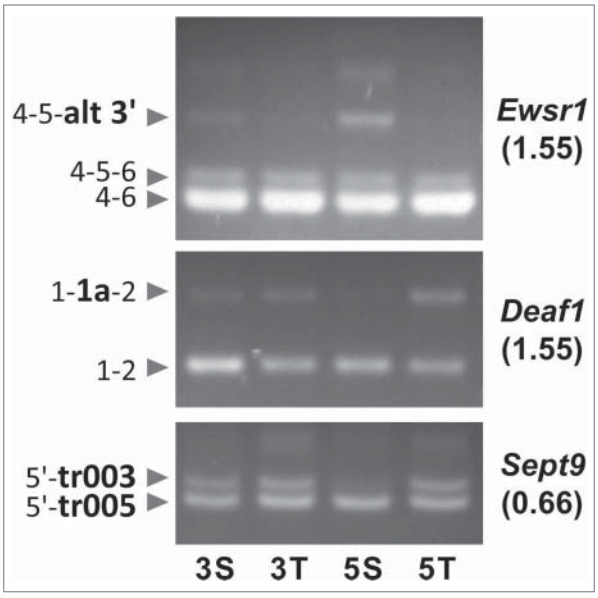

Figure 4. Prolonged SMN depletion in NB2a cells leads to more extensive splicing alterations. Mouse NB2a cells were depleted of SMN or TCRβ for 3 and 5 days, and the splicing of the gene region of interest was analyzed by RT-PCR as described in the legend of **Figure 2**. Numbers in brackets below the gene symbols represent the fold change in probe inclusion (dI) in SMA mice as calculated from the microarray data (1 = equal inclusion). The exons contained in the amplified products are indicated on the left with alternative exons shown in larger font size and bold letters; alt 3′: alternative 3′ exon; a: alternative exon. For *Sept9*, the assay detects a switch between the alternative 5′ exons of the transcripts 003 and 005.

and that disease-induced splicing changes in MNs may be obscured and escape detection when one looks at RNA from whole spinal cord.

What is the importance of major and minor spliceosomes for SMA?

An important discussion in the field concerns the relative contributions of the 2 spliceosomal systems (U2 vs. U12) to SMA pathogenesis. The idea that the minor spliceosome may be particularly important for SMA was put forth, because measurements of U snRNA concentrations in cellular SMN depletion systems and tissues of SMA mice had revealed a stronger reduction in snRNAs of the U12-spliceosome.[17,38,42]

Contrasting with this notion, the transcriptome studies carried out on different SMA models,[38-41,43] including our own study, have revealed numerous alterations in U2-dependent splicing events, but none in U12-dependent events. As mentioned previously, this may partly be due to a bias of the analytical systems. Deficiencies in U12-dependent splicing events are usually manifested by intron retention or by a decrease in transcript levels, because the intron-containing RNA variants are subject to NMD. Such events might not be efficiently detected by any method, be it exon or exon junction arrays or deep RNA sequencing.

The experimental system of SMN-depleted NB2a cells which we used for our validations helped to shed some light on this question, as it allowed us to study splicing changes for a relatively large set of genes. Most importantly, we could study the partial SMN depletion while it progressed from an early, moderate to a later, more extensive stage. Even though this system revealed a number of differences compared to MNs, it has provided valuable information regarding the types of genes and introns affected by SMN depletion.

Altogether, the NB2a system allowed us to detect more than 22 changes in U2-dependent splicing events and 5 changes in U12-introns. After 3 d of SMN depletion, with 15–20% of SMN mRNA and protein remaining, all 22 U2-dependent splicing events listed in **Table 2** were altered. After 5 d of depletion, with an SMN reduction to 5–10%, several of these changes became more pronounced, and additional ones were detectable (**Fig. 4**). In contrast, the 5 observed U12-dependent splicing changes (out of 12 testable events) only became detectable by conventional RT-PCR at 5 d of SMN depletion (**Fig. 5**). At 3 d of depletion, slight reductions in *Ap4m1* and *Tmem41b* transcript levels could be measured by RT-qPCR, but, for *Tmem41b*, this reduction was only marginally significant. Moreover, our qPCR measurements of U snRNAs suggested that 5 d of SMN depletion in NB2a cells are required for reductions in the levels of multiple U snRNAs to become apparent (**Fig. S2** of Supplementary File 2). However, these measurements did not provide evidence for a preferential reduction of minor U snRNAs. Taken together, our results therefore indicate that U2-dependent splicing events are affected earlier than those of the minor U12 spliceosome, at least in these NB2a cells.

Altogether, the U snRNA expression profile after 5 d of SMN depletion looked more similar to those published for other SMN-depleted cell models and SMA mouse tissues[17,38,42] than the one after 3 d of depletion. Multiple snRNAs were reduced, although we cannot conclude from our data that this reduction was stronger for snRNAs of the minor spliceosome compared to those of the major one. It is possible that the extent to which different U snRNA levels are affected by a SMN deficiency may vary between cellular systems (see Zhang et al. 2008[38] for examples). However, based on our data, we think that the situation presented in previous studies, where most snRNAs showed a reduction and some of the minor spliceosomal components were most strongly affected,[17,38,42] may reflect a point in time well beyond the first occurrences of splicing defects.

Unfortunately it has not been tested, in any biological system, when the first splicing changes occur in response to a reduced SMN concentration and whether snRNP levels are significantly reduced at this time point. In other words, it is still not clear whether reduced snRNP assembly and reduced snRNP levels are indeed the cause for these first splicing defects. As mentioned in the Introduction, there is supporting evidence for this hypothesis. Thus, the snRNP assembly activity of certain SMN point mutations was found to correlate with disease severity in transgenic mouse models.[17,18] Moreover, MN growth defects induced in zebrafish embryos by antisense oligonucleotide-mediated SMN

depletion could be prevented by injecting snRNPs isolated from HeLa cells.[19] Nevertheless, a firm proof for the idea that these splicing changes are indeed caused by low snRNP levels in SMA patients or in animal models which recapitulate the human situation is missing. Thus one should at least entertain the alternative possibility that SMN may cause splicing changes by a different mechanism, e.g., by affecting the metabolism or function of other splicing factors such as SR and hnRNP proteins which are key regulators of alternative splicing.[61,62]

Genes affected and their possible relationship to SMA pathogenesis

An important motivation for this study was to gain insight into pathogenic mechanisms leading to SMA through the identification of genes whose splicing, or more generally whose expression, is altered. When we consider those genes whose splicing changes were confirmed in NB2a cells after 3 d of SMN depletion (**Table 2**), these fall into 3 main functional categories:

1. Cellular and developmental/neuronal functions (*Ank2*, *Afiph*, *Atp11c*, *Pkp4*, *Rltpr*, *Sept9*)
2. Transcription and growth control (*Deaf1*, *E2f6*, *Igf1*, *Mtf2*, *Pdcd2l*, *Plag1*, *Src*, *Supt20h*)
3. RNA metabolism, especially splicing (*Clk3*, *Cstf2*, *Ewsr1*, *Pum1*, *Rbfox1/A2bp1*, *Scaf8/Rbm16*, *Tia1*, *Ythdc1*)

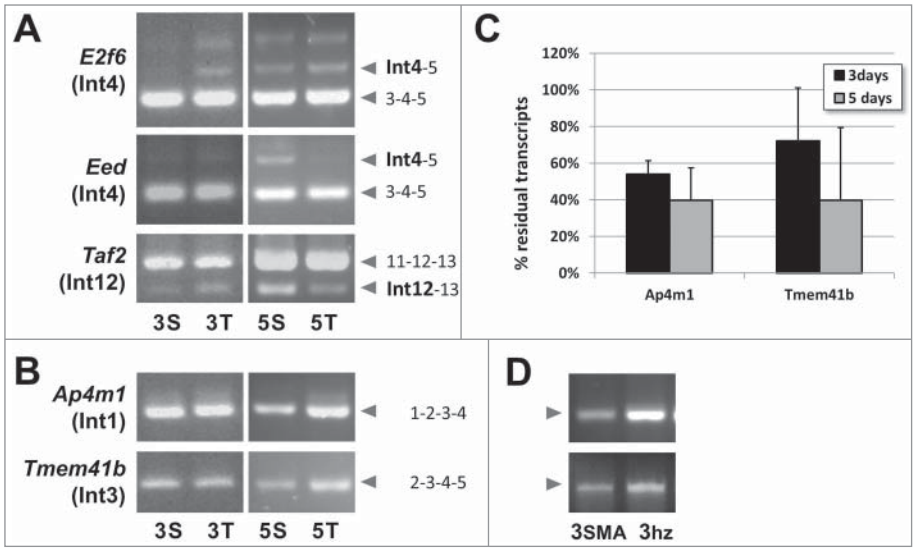

Figure 5. Evidence for U12 intron retention after prolonged SMN depletion in NB2a cells and in SMA mouse motoneurons. (**A**) Examples showing intron retention in NB2a cells. The cells were depleted of SMN or TCRβ, and the splicing of the gene region of interest was analyzed by RT-PCR as described in the legend of **Figure 2**. The labeling on the side of the gels indicates the exons partly or fully amplified by this assay. Parts of retained U12 introns are indicated in bold and larger font size. The U12 intron of interest is also mentioned between brackets following the gene symbol. Note that the introns 4 of *Eed* and 12 of *Taf2*, but not the *E2f6* intron 4, accumulate after 5 d of SMN depletion. (**B**) Reduction of *Ap4m1* and *Tmem41b* transcript levels after SMN depletion in NB2a cells. The missing transcripts have most likely been degraded by nonsense-mediated mRNA decay because of stop codons in the retained U12 intron. (**C**) RT-qPCR analysis of *Ap4m1* and *Tmem41b* transcript levels in SMN depleted NB2a cells. Error bars represent standard deviations. P values for 2-sided Student T test (N = 4): *Ap4m1*, 3S vs. 3T, 1.6×10^{-5}, 5S vs. 5T, 4.8×10^{-4}, 3S vs. 5S, 0.19; *Tmem41b*, 3S vs. 3T, 0.041, 5S vs. 5T, 0.023, 3S vs. 5S, 0.35. (**D**) Reduction of *Ap4m1* and *Tmem41b* transcript levels in LCM-isolated MNs from P3 SMA mice (3SMA) compared to heterozygous mice (3hz). The experiments were performed with the same cDNA preparation for which results of other genes including the SMN depletion control and the 5.8S rRNA loading control have been shown in **Figure 3**.

Even though the selection of genes for our validation attempts was somewhat biased, it is clear from this list that important functions for any cell, and especially for neuronal cells, are affected. A gene ontology analysis performed on the entire set of strong splicing changes resulted in a similar picture (Tab 3 of the Supplementary File 1; also see descriptions in first part of the results). Moreover, one of the 3 splicing events which were altered in our study and in MNs from Δ7 mice at P1[43] affects the *Gria2* gene that codes for the glutamate receptor 2, while the other 2 concern genes for potential transcription/RNA processing regulators (*Scaf8/Rbm16* and *Zfp821*). The *Gria2* transcripts are known to be edited by adenine deamination, and a reduction of this editing has been observed in the motoneuron disease Amyotrophic Lateral Sclerosis (ALS).[63,64] This could be an interesting cue to follow up in further studies.

Another one of the strongly regulated genes from our analysis which was also identified in the whole spinal cord microarray studies of Zhang et al. 2008[38] and Bäumer et al.[39] is *Uspl1*. The splicing of this gene has also been used as tracer in a recent study on various stages of SMA mice.[65] Its protein product, according to the GeneCards database, is involved in the desumoylation of proteins.

A few other genes for which we have detected splicing changes in our MN microarrays may also contribute to the pathology of the disease. For example, *Eed*, a member of the polycomb family has been linked to deficient growth in stem cells.[66] This could be interesting, because a recent study in *Drosophila* has demonstrated an influence of SMN on stem cell division, proliferation and differentiation.[33] Besides *Eed*, *E2f6* is another putative member of the polycomb complex. In the case of mouse MNs, *E2f6* has a single transcript which codes for a truncated protein; it is not known whether this could have any function. Furthermore, the mouse *Igf1* Ec splicing isoform was reduced at 3 d of SMN depletion in NB2a cells. The Ec isoform has been reported to play a neuro-protective role.[67,68] Finally, as shown in **Figure 5**, the transcripts coding for Tmem41b, a vital protein required for maintaining the excitability of MNs,[42,69] appear to be degraded via NMD due to aberrant splicing of a U12-intron.

Table 3. List of SMA-associated splicing changes identified in multiple studies.

Study		this paper	Ref. 43	Ref. 39	Ref. 39	Ref. 38	Ref. 39
Model		severe	Δ7	Δ7	Δ7	Δ7	Δ7
stage		P3	P1	P1	P7	P11	P13
sample origin		motoneurons	motoneurons	spinal cord	spinal cord	spinal cord	spinal cord
method		EJA	NGS	EA	EA	EA	EA
Gene symbol	Gene name						
1700007K13Rik	Gene for Riken cDNA 1700007K13				✓		✓
Agrn	Agrin		?			?	
Atg9b	Autophagy Related 9B					✓	✓
Calcb	Calcitonin Gene-Related Peptide 2, beta-CGRP				✓		✓
Cdkn1a	Cyclin-Dependent Kinase Inhibitor 1				✓	?	✓
Chodl	Chondrolectin				✓	?	✓
Dcxr	Dicarbonyl/L-Xylulose Reductase				✓	?	✓
Gna14	Guanine Nucleotide Binding Protein (G Protein) Alpha 14				✓	?	✓
Gria2	Glutamate Receptor, Ionotropic, AMPA 2	?	?				
Hif3a	Hypoxia Inducible Factor 3, Alpha Subunit					?	?
Id4	Inhibitor Of DNA Binding 4, Dominant Negative Helix-Loop-Helix protein					✓	✓
Mapk4	Mitogen-Activated Protein Kinase 4					✓	✓
Mccc2	Methylcrotonoyl-CoA Carboxylase 2 (Beta)			✓	✓		
Phactr3	Phosphatase And Actin Regulator 3					?	?
Plk2	Polo-Like Kinase 2				✓		✓
Polk	Polymerase (DNA Directed) Kappa					?	?
Polr3e	Polymerase (RNA) III (DNA Directed) Polypeptide E (80kD)					✓	✓
Psrc1	Proline/Serine-Rich Coiled-Coil 1				✓		✓
Ptk2b	Protein Tyrosine Kinase 2 Beta					?	?
Rbm6	RNA Binding Motif Protein 6	✓	✓				
Rgs12	Regulator Of G-Protein Signaling 12				✓		✓
Sept9	Septin 9	?				?	
Smn1				✓	✓		✓
Snrpa1	Small Nuclear Ribonucleoprotein Polypeptide A	no		✓	✓		✓
Stx3	Syntaxin 3	?		?			
Sult1a1	Sulfotransferase Family, Cytosolic, 1A, Phenol-Preferring, Member 1				✓	no	✓
Tesc	Tescalcin				✓		✓
Trim7	Tripartite Motif Containing 7					?	?
Uspl1	Ubiquitin Specific Peptidase Like 1	✓		✓	✓	✓	
Zfp821	Zinc Finger Protein 821	✓	✓				
	Total matches	7	4	5	15	17	22
	Total entries	477	104	72	67	259	812
	% matches	1.47%	3.85%	6.94%	22.39%	6.56%	2.71%

A clustering of matches between this paper and Ref. 43 as well as between the studies of Refs 38 and 39 is indicated by stronger cell separations. EJA, exon junction array; NGS, next generation sequencing; EA, exon array; ✓, full match, identical exons or splicing events affected; ?, possible match, usually affecting adjacent exons that might be involved in the same splicing change.

Despite the fact that the outcome of the splicing changes on the encoded proteins has not been determined experimentally and is sometimes difficult to predict based on gene structure, all these and several of the other detected changes are potentially very important for cell physiology and MN function. However, it is difficult to identify which changes are primary ones, which ones are particularly important for the development of the disease state and which ones may simply be consequences of a disturbed cell physiology without much significance for SMA pathogenesis. Similar studies in earlier stages, i.e. in mouse fetuses and perinatal stages, might help to shed some light on these questions. However, the isolation of MNs in sufficient quantity and quality will be technically more demanding for such early stages.

Table 4. Summary of SMA-associated splicing changes identified in multiple studies.

Study	this paper	Ref. 43	Ref. 39	Ref. 39	Ref. 38	Ref. 39
Model	severe	Δ7	Δ7	Δ7	Δ7	Δ7
stage	P3	P1	P1	P7	P11	P13
samples	motoneurons	motoneurons	spinal cord	spinal cord	spinal cord	spinal cord
method	EJA	NGS	EA	EA	EA	EA
this paper		3	2	1	2	0
Ref. 43, P1	3		0	0	1	0
Ref. 39, P1	2	0		4	1	2
Ref. 39, P7	1	0	4		5	13
Ref. 38, P11	2	1	1	5		13
Ref. 39, P13	0	0	2	13	13	

A clustering of matches between this paper and Ref. 43 as well as between the studies of Refs 38 and 39 is indicated by grey shading and stronger cell separations. EJA, exon junction array; NGS, next generation sequencing; EA, exon array.

One advantage of our study, was that we could not only compare SMA mice to healthy heterozygotes, but also to SMA/U7 mice in which a therapeutic U7 gene partly corrects *SMN2* exon 7 splicing, and hence the SMA phenotype.[44] The fact that, overall, the strongly altered splicing events were reversed in SMA/U7 mice indicates that most of them are indeed associated with the SMA genotype. However, as the SMA/U7 mice inherited the therapeutic U7 gene at conception, the U7 gene should have caused a correction of all changes, regardless of whether they are primary or secondary ones.

Altered expression of RNA processing regulators may aggravate SMA-induced missplicing

One of the most important results of our study is that several genes which showed splicing defects encode splicing and 3' end processing factors or proteins that regulate the activity of RNA processing factors (*Clk3*, *Cstf2*, *Rbfox1/A2bp1*, *Scaf8/Rbm16*, *Tia1*, *Ythdc1*). Changes in this group of proteins may therefore amplify the alternative splicing that is primarily induced by low levels of SMN, or they may even feedback on the splicing of the *SMN2* gene. In particular, Tia1 has recently been identified as a positive regulator of *SMN2* exon7 splicing, so that a loss of Tia1 may contribute to a negative feedback loop that reinforces exon7 skipping.[70] Together with new evidence showing that the production of functional SMN protein from *SMN2* was lower in the MNs of SMA mice than in other types of neurons of the spinal cord,[14] a dysregulation of Tia1 that has been shown to be important for SMN exon 7 inclusion[71] could at least partly explain the extra vulnerability of MNs in SMA. Additionally, *Clk3* encodes a serine/threonine type protein kinase that regulates the intranuclear distribution of the SR family of splicing factors.[72] In principle, for each of these RNA processing regulators, a change in its level or activity may induce a secondary wave of splicing defects which supersedes the one caused by reduced SMN levels and altered snRNP assembly or metabolism. In other words, we should perceive the monogenic defect of SMN to be the seed for a chain reaction of splicing defects in SMA.

Materials and Methods

Plasmids and lentiviral constructs

Plasmids were cloned in *E. coli* strain XL10 Gold and amplified with chloramphenicol (final concentration 170μg/ml; added during a second day of incubation).

Short hairpin (sh) RNA sequences targeting mouse *SMN* were cloned as double-stranded oligonucleotides between BglII and HindIII restriction sites, downstream of the H1 promoter, in a pSUPERpuro[73] derivative that contains a 1834bps stuffer fragment (pSUPuro-sL) between these sites. Thus the stuffer fragment was replaced by the shRNA sequence. Multiple shRNAs were generated, but the one used for these experiments targets the sequence GAAGTAAAGCACACAGCAA in exon 4 (i.e., the fifth exon, as 2 exons are named 2a and 2b). As negative control, a pSUPERpuro shRNA construct targeting T cell receptor β (TcRβ; which should not be expressed in the cells of interest) was used.[74] These pSUPERpuro vectors contain a puromycin resistance gene that allows for rapid selection of transiently transfected cells.

Cell culture and transient transfections

NB2a cells were maintained at 5% CO_2 and 37°C in DMEM supplemented with 10% fetal calf serum (FCS; Sigma), 100U/ml penicillin, 100 μg/ml streptomycin and 2mM L-glutamine (all from Amimed). For transient transfection, ~2.5×10^5 cells were seeded per well (6-well plate) and incubated overnight. The medium was replaced by serum- and antibiotics-free medium for 1 hour pre-transfection. Complexes of DNA plasmids and FuGENE transfection reagent (Promega E2312) were formed and applied to cells dropwise. Complete medium was added back to the cells 6–8 hours post-transfection. In microarray RT-PCR validation experiments, 1.5 μg of pSUPuro constructs were dosed per transfection, and continuous puromycin selection (final concentration 2.25 μg/ml) followed till harvest.

Animal breeding and tissue dissection

The severe SMA mouse model (*mSmn* -/-; *hSMN2* +/+) (Jackson Laboratory 005024);[45] which generally survives 6–8 d

was used in this study. New born mice were genotyped[44] on the day of birth (P0), and dissection was carried out at P3. Spinal cords were harvested from mice of either SMA (*mSmn −/−; hSMN2+/+*) or carrier (*mSmn +/−; hSMN2+/+*) genotype. Additionally, we used SMA animals with multiple copies of a U7-ESE-B1 transgene that partly corrects the splicing of SMN2 exon 7 and suppresses the SMA phenotype (*mSmn −/−; hSMN2+/+; U7-ESE-B1*).[44] The animals were kept at the central animal house of Insel hospital and handled according to Swiss animal protection law under the permissions BE 102/06, BE 5/10 and BE 14/13.

Laser capture micro-dissection (LCM), exon junction microarray and data mining

The lumbar region of the spinal cord was isolated and embedded in O.C.T compound for storage at −80°C. To prepare for LCM, the embedded sample was cut into 30 μm slices in a cryostat and transferred onto membrane slides (MMI 50102). Samples were stained with methylene blue (Sigma 03978), and subsequently destained/dehydrated in absolute ethanol. MMI CellCut (Molecular Machines & Industries, Glattbrugg, Switzerland) and PALM Microbeam (Zeiss) LCM systems were used to collect the MN samples for microarray hybridization and validation, respectively. MN cell bodies were collected rapidly in LCM isolation caps (MMI 50202) and immediately stabilised in the Picopure RNA isolation kit extraction buffer (AppliedBiosystems KIT0204).

The RNA extraction was performed with the Picopure RNA isolation kit, and samples were subjected to on-column DNase treatment. The quality and integrity of obtained RNA was then analyzed with a 2100 Bioanalyser (Agilent). Only RNAs with clearly visible large rRNA bands were used. The RNA input was standardised before reverse transcription (RT) and cDNA amplification with Oviation Pico WTA system (Nugen 3300) kits or the later version V2 (Nugen 3302).

Affymetrix exon-junction microarray chips and MN samples were processed at the Friedrich Miescher Institute functional genomic facility where RNA isolation, quantification, cDNA amplification and chip hybridization were carried out. The scanned chip images were analyzed by M.K. in the lab of J.U. at the MRC-LMB in Cambridge. The analysis of microarray data was done with ASPIRE version 3 (Analysis of SPlicing Isoform REciprocity) software as described earlier.[48] ASPIRE3 predicts splicing changes from reciprocal probe sets that recognize either inclusion or skipping of an alternative exon. Background subtraction and ranking of predicted splicing changes are done during the analysis. The original CEL files have been deposited in the ArrayExpress database at EBI (http://www.ebi.ac.uk/arrayexpress/; accession number E-MTAB-3170).

RNA extraction

Total RNA from cultured cells was extracted with homemade Tri-Reagent[75] and resuspended in diethyl pyrocarbonate-treated water. Mouse tissues samples were either chopped into small pieces or snap frozen, and then crushed with a pestle (BioConcept 100539). The RNA was then extracted with an RNeasy mini kit (Qiagen 74104). All isolated RNA samples were subjected to DNase I treatment (Roche 04716728001). The RNA quantity and integrity were checked by Nanodrop 2000 spectrophotometer and gel electrophoresis, respectively. Only RNAs with clearly visible large rRNA bands were used and RNA inputs were standardised for RT-PCR analyses.

Splicing analysis by RT-PCR and band sequencing

The Ensembl (Archive site Feb 2011) and Aceview databases were used to study the region of interest corresponding to microarray probes. Based on these informations, primers were designed and checked for specificity by BLAST (http://www.ncbi.nlm.nih.gov/tools/primer-blast/). Primers were purchased from Microsynth (Balgach, Switzerland). Primers specific for 5.8S rRNA and for mouse SMN mRNA were used to control equal inputs and SMN depletion, respectively.

For reverse transcription (RT), 3 μg of isolated RNA was incubated with reverse transcriptase (Agilent 60010951), and both oligo dT and random primers were included in the reactions. The RT reactions were performed at 42°C for 1 hour, and the enzyme was inactivated at 85°C.

PCR reactions were performed on an Eppendorf mastercycler. The cycles generally consisted of denaturation at 95°C and annealing at 55°C (or at an optimised temperature as tested by gradient PCR) in Faststart PCR mastermix (Roche 04710444001). The numbers of PCR cycles were adjusted according to the abundance of transcripts detected in the various samples. To clone and sequence individual PCR products, amplifications (20 cycles) were carried out with PfuUltra High-Fidelity DNA polymerase (Agilent 600387), DNA bands of interest were excised from agarose gels, purified and cloned into pGEM-T Easy vector (Promega A1360). Mini-prep DNA was sequenced through either an in-house sequencing service (Appliedbiosystems ABI 3100) or by Microsynth (Balgach, Switzerland).

Real-time quantitative RT-PCR analysis

The real-time quantitative RT-PCR experiments were performed by following the minimum information for publication of quantitative real-time PCR experiment (MIQE) guidelines.[76] The reactions were analyzed on a Rotor-Gene Q real-time PCR cycler (Qiagen). Each PCR program performed 40 cycles of amplification, consisting of a 15 sec denaturing step at 95°C, 15 sec annealing at 60°C, and 20 sec extension at 72°C. The recording range of the melting curve was set from 70°C to 95°C. For each experimental variant, several independent experiments were performed, and all samples were measured in duplicates. Based on a list of coding and non-coding[77] genes, additional data from the literature and our own initial experiments, we selected the non-coding 7SK RNA as the most suitable reference gene to normalize the qPCR data. After normalization for this reference, $\Delta\Delta C_T$ values and fold changes of the measured RNAs were calculated.

Western blots and antibodies

Cells were lysed in home-made RIPA buffer [150 mM NaCl, 0.1% NP-40, 0.5% sodium deoxycholate, 50mM Tris (pH = 8 .0)] supplemented with protease inhibitor cocktail (Calbiochem 539134) and 1mM DTT. The lysates were subjected to Dounce

homogenization on ice, and the soluble fraction was obtained by 12,000g centrifugation, aliquoted and snap frozen. The protein concentration of samples was determined by BCA protein assay kit (Pierce 23225).

Soluble proteins were separated on 10% SDS-polyacrylamide gels and transferred onto Immobilon-FL PVDF membrane (Millipore IPFL00010). A solution of 5% milk powder was applied to the membranes as blocking solution for 1 hour at room temperature. Blots were incubated with primary antibodies at 4°C overnight. Rabbit antibody against mouse Smn[44] and mouse anti-α tubulin antibody (developmental studies hybridoma bank AA 4.3-s) were diluted 1:1'000 and 1:4'000, respectively. Both secondary antibodies donkey anti-mouse 800cw (Odyssey IRDye 92632212) and donkey anti-rabbit 680 (Odyssey IRDye 92632221) were used at a dilution factor of 1:10'000, and their co-incubations with blots were performed in the dark. TBST buffer (10 nM Tris, pH 7.5, 150 mM NaCl, 0.05% Tween 20) was used for interval washes. An Odyssey infrared imaging system (Licor) was used to scan blot membranes and quantify proteins of interest.

Disclosure of Potential Conflicts of Interest

No potential conflicts of interest were disclosed.

Acknowledgments

We thank Judith Trüb for excellent technical help and for maintaining our mouse colony, Pierre de la Grange (GenoSplice, Evry, F) for additional bioinformatic help, the lab of Didier Trono (EPFL Lausanne) for lentiviral vectors, Pico Caroni (Friedrich Miescher Institute, Basel) and Christoph Müller (Pathology Institute, University of Bern) for permission to use LCM microscopes and other equipment and services at their institutes.

Funding

This work was supported by the Swiss National Science Foundation (grants 31003A-120064 and 31003A-135644), the Swiss Foundation for Research on Muscle Diseases, EURASNET (European Network of Excellence on Alternative Splicing), AFM (Association Française contre les Myopathies), and the Kanton Bern.

Supplemental Material

Supplemental data for this article can be accessed on the pub lisher's website.

References

1. Pearn J. Incidence, prevalence, and gene frequency studies of chronic childhood spinal muscular atrophy. J Med Genet 1978; 15:409-13; PMID:745211; http://dx.doi.org/10.1136/jmg.15.6.409
2. Ogino S, Wilson RB. Spinal muscular atrophy: molecular genetics and diagnostics. Expert Rev Mol Diagn 2004; 4:15-29; PMID:14711346; http://dx.doi.org/10.1586/14737159.4.1.15
3. Lunn MR, Wang CH. Spinal muscular atrophy. Lancet 2008; 371:2120-33; PMID:18572081; http://dx.doi.org/10.1016/S0140-6736(08)60921-6
4. Sugarman EA, Nagan N, Zhu H, Akmaev VR, Zhou Z, Rohlfs EM, Flynn K, Hendrickson BC, Scholl T, Sirko-Osadsa DA, et al. Pan-ethnic carrier screening and prenatal diagnosis for spinal muscular atrophy: clinical laboratory analysis of >72 ; [thinsp]400 specimens. Eur J Hum Genet 2012; 20:27-32; PMID:21811307; http://dx.doi.org/10.1038/ejhg.2011.134
5. Lefebvre S, Burglen L, Reboullet S, Clermont O, Burlet P, Viollet L, Benichou B, Cruaud C, Millasseau P, Zeviani M. Identification and characterization of a spinal muscular atrophy-determining gene. Cell 1995; 80:155-65; PMID:7813012; http://dx.doi.org/10.1016/0092-8674(95)90460-3
6. Lorson CL, Hahnen E, Androphy EJ, Wirth B. A single nucleotide in the SMN gene regulates splicing and is responsible for spinal muscular atrophy. Proc Natl Acad Sci U S A 1999; 96:6307-11; PMID:10339583; http://dx.doi.org/10.1073/pnas.96.11.6307
7. Lorson CL, Androphy EJ. An exonic enhancer is required for inclusion of an essential exon in the SMA-determining gene SMN. Hum Mol Genet 2000; 9:259-65; PMID:10607836; http://dx.doi.org/10.1093/hmg/9.2.259
8. Cartegni L, Krainer AR. Disruption of an SF2/ASF-dependent exonic splicing enhancer in SMN2 causes spinal muscular atrophy in the absence of SMN1. Nat Genet 2002; 30:377-84; PMID:11925564; http://dx.doi.org/10.1038/ng854
9. Cartegni L, Hastings ML, Calarco JA, de Stanchina E, Krainer AR. Determinants of exon 7 splicing in the spinal muscular atrophy genes, SMN1 and SMN2. Am J Hum Genet 2006; 78:63-77; PMID:16385450; http://dx.doi.org/10.1086/498853
10. Kashima T, Rao N, Manley JL. An intronic element contributes to splicing repression in spinal muscular atrophy. Proc Nat Acad Sci U S A 2007; 104:3426-31; PMID:17307868; http://dx.doi.org/10.1073/pnas.0700343104
11. Fischer U, Englbrecht C, Chari A. Biogenesis of spliceosomal small nuclear ribonucleoproteins. Wiley Interdiscip Rev RNA 2011; 2:718-31; PMID:21823231; http://dx.doi.org/10.1002/wrna.87
12. Burghes AHM, Beattie CE. Spinal muscular atrophy: why do low levels of survival motor neuron protein make motor neurons sick? Nat Rev Neurosci 2009; 10:597-609; PMID:19584893; http://dx.doi.org/10.1038/nrn2670
13. Sleeman J. Small nuclear RNAs and mRNAs: linking RNA processing and transport to spinal muscular atrophy. Biochem Soc Trans 2013; 41:871-5; PMID:23863147; http://dx.doi.org/10.1042/BST20120016
14. Ruggiu M, McGovern VL, Lotti F, Saieva L, Li DK, Kariya S, Monani UR, Burghes AH, Pellizzoni L. A role for SMN exon 7 splicing in the selective vulnerability of motor neurons in spinal muscular atrophy. Mol Cell Biol 2012; 32:126-38; PMID:22037760; http://dx.doi.org/10.1128/MCB.06077-11
15. Boulisfane N, Choleza M, Rage F, Neel H, Soret J, Bordonné R. Impaired minor tri-snRNP assembly generates differential splicing defects of U12-type introns in lymphoblasts derived from a type I SMA patient. Hum Mol Genet 2011; 20:641-8; PMID:21098506; http://dx.doi.org/10.1093/hmg/ddq508
16. Clelland AK, Bales ABE, Sleeman JE. Changes in intranuclear mobility of mature snRNPs provide a mechanism for splicing defects in spinal muscular atrophy. J Cell Sci 2012; 125:2626-37; PMID:22393244; http://dx.doi.org/10.1242/jcs.096867
17. Gabanella F, Butchbach MER, Saieva L, Carissimi C, Burghes AHM, Pellizzoni L. Ribonucleoprotein assembly defects correlate with spinal muscular atrophy severity and preferentially affect a subset of spliceosomal snRNPs. P L S ONE 2007; 2:e921; PMID:17895963
18. Workman E, Saieva L, Carrel TL, Crawford TO, Liu D, Lutz C, Beattie CE, Pellizzoni L, Burghes AH. A SMN missense mutation complements SMN2 restoring snRNPs and rescuing SMA mice. Hum Mol Genet 2009; 18:2215-29; PMID:19329542; http://dx.doi.org/10.1093/hmg/ddp157
19. Winkler C, Eggert C, Gradl D, Meister G, Giegerich M, Wedlich D, Laggerbauer B, Fischer U. Reduced U snRNP assembly causes motor axon degeneration in an animal model for spinal muscular atrophy. Genes Dev 2005; 19:2320-30; PMID:16204184; http://dx.doi.org/10.1101/gad.342005
20. Terns MP, Terns RM. Macromolecular complexes: SMN–the master assembler. Curr Biol 2001; 11:R862-R4; PMID:11696342; http://dx.doi.org/10.1016/S0960-9822(01)00517-6
21. Bachand F, Boisvert FM, Cote J, Richard S, Autexier C. The product of the survival of motor neuron (SMN) gene is a human telomerase-associated protein. Mol Biol Cell 2002; 13:3192-202; PMID:12221125; http://dx.doi.org/10.1091/mbc.E02-04-0216
22. Piazzon N, Schlotter F, Lefebvre S, Dodré M, Méreau A, Soret J, Besse A, Barkats M, Bordonné R, Branlant C, et al. Implication of the SMN complex in the biogenesis and steady state level of the signal recognition particle. Nucleic Acids Res 2013; 41:1255-72; PMID:23221635; http://dx.doi.org/10.1093/nar/gks1224
23. Peter CJ, Evans M, Thayanithy V, Taniguchi-Ishigaki N, Bach I, Kolpak A, Bassell GJ, Rossoll W, Lorson CL, Bao ZZ, et al. The COPI vesicle complex binds and moves with survival motor neuron within axons. Hum Mol Genet 2011; 20:1701-11; PMID:21300694; http://dx.doi.org/10.1093/hmg/ddr046
24. Ting C-H, Wen H-L, Liu H-C, Hsieh-Li H-M, Li H, Lin-Chao S. The spinal muscular atrophy disease protein SMN is linked to the golgi network. PLoS ONE 2012; 7:e51826; PMID:23284781; http://dx.doi.org/10.1371/journal.pone.0051826
25. Kerr DA, Nery JP, Traystman RJ, Chau BN, Hardwick JM. Survival motor neuron protein modulates neuron-specific apoptosis. Proc Nat Acad Sci U S A 2000; 97:13312-7; PMID:11078511; http://dx.doi.org/10.1073/pnas.230364197
26. Parker GC, Li X, Anguelov RA, Toth G, Cristescu A, Acsadi G. Survival motor neuron protein regulates

apoptosis in an in vitro model of spinal muscular atrophy. Neurotox Res 2008; 13:39-48; PMID:18367439; http://dx.doi.org/10.1007/BF03033366
27. Sareen D, Ebert AD, Heins BM, McGivern JV, Ornelas L, Svendsen CN. Inhibition of apoptosis blocks human motor neuron cell death in a stem cell model of spinal muscular atrophy. PloS one 2012; 7:e39113; PMID:22723941; http://dx.doi.org/10.1371/journal.pone.0039113
28. Anderton RS, Price LL, Turner BJ, Meloni BP, Mitrpant C, Mastaglia FL, Goh C, Wilton SD, Boulos S. Co-regulation of survival of motor neuron and Bcl¯xL expression: implications for neuroprotection in spinal muscular atrophy. Neuroscience 2012; 220:228-36; PMID:22732506; http://dx.doi.org/10.1016/j.neuroscience.2012.06.042
29. Zou J, Barahmand-pour F, Blackburn ML, Matsui Y, Chansky HA, Yang L. Survival motor neuron (SMN) protein interacts with transcription corepressor mSin3A. J Biol Chem 2004; 279:14922-8; PMID:14749338; http://dx.doi.org/10.1074/jbc.M309218200
30. Fan L, Simard LR. Survival motor neuron (SMN) protein: role in neurite outgrowth and neuromuscular maturation during neuronal differentiation and development. Hum Mol Genet 2002; 11:1605-14; PMID:12075005; http://dx.doi.org/10.1093/hmg/11.14.1605
31. Giavazzi A, Setola V, Simonati A, Battaglia G. Neuronal-specific roles of the survival motor neuron protein: evidence from survival motor neuron expression patterns in the developing human central nervous system. J Neuropathol Exp Neurol 2006; 65:267-77; PMID:16651888; http://dx.doi.org/10.1097/01.jnen.0000205144.54457.a3
32. Bosio Y, Berto G, Camera P, Bianchi F, Ambrogio C, Claus P, Di Cunto F. PPP4R2 regulates neuronal cell differentiation and survival, functionally cooperating with SMN. Europ J Cell Biol 2012; 91:662-74; PMID:22559936; http://dx.doi.org/10.1016/j.ejcb.2012.03.002
33. Grice SJ, Liu JL. Survival motor neuron protein regulates stem cell division, proliferation, and differentiation in drosophila. PLoS genetics 2011; 7:e1002030; PMID:21490958; http://dx.doi.org/10.1371/journal.pgen.1002030
34. Kariya S, Park GH, Maeno-Hikichi Y, Leykekhman O, Lutz C, Arkovitz MS, Landmesser LT, Monani UR. Reduced SMN protein impairs maturation of the neuromuscular junctions in mouse models of spinal muscular atrophy. Hum Mol Genet 2008; 17:2552-69; PMID:18492800; http://dx.doi.org/10.1093/hmg/ddn156
35. Dachs E, Hereu M, Piedrafita L, Casanovas A, Calderó J, Esquerda JE. Defective neuromuscular junction organization and postnatal myogenesis in mice with severe spinal muscular atrophy. J Neuropathol Exp Neurol 2011; 70:444-61; PMID:21572339; http://dx.doi.org/10.1097/NEN.0b013e31821cbd8b
36. Lee Yi, Mikesh M, Smith I, Rimer M, Thompson W. Muscles in a mouse model of spinal muscular atrophy show profound defects in neuromuscular development even in the absence of failure in neuromuscular transmission or loss of motor neurons. Dev Biol 2011; 356:432-44; PMID:21658376; http://dx.doi.org/10.1016/j.ydbio.2011.05.667
37. Martínez-Hernández R, Bernal S, Also-Rallo E, Alías L, Barceló M, Hereu M, Esquerda JE, Tizzano EF. Synaptic defects in type I spinal muscular atrophy in human development. J Pathol 2013; 229:49-61; PMID:22847626; http://dx.doi.org/10.1002/path.4080
38. Zhang Z, Lotti F, Dittmar K, Younis I, Wan L, Kasim M, Dreyfuss G. SMN Deficiency causes tissue-specific perturbations in the repertoire of snRNAs and widespread defects in splicing. Cell 2008; 133:585-600; PMID:18485868; http://dx.doi.org/10.1016/j.cell.2008.03.031
39. Baumer D, Lee S, Nicholson G, Davies JL, Parkinson NJ, Murray LM, Gillingwater TH, Ansorge O, Davies KE, Talbot K. Alternative splicing events are a late feature of pathology in a mouse model of spinal muscular atrophy. PLoS Genet 2009; 5:e1000773; PMID:20019802; http://dx.doi.org/10.1371/journal.pgen.1000773
40. Murray LM, Lee S, Baumer D, Parson SH, Talbot K, Gillingwater TH. Pre-symptomatic development of lower motor neuron connectivity in a mouse model of severe spinal muscular atrophy. Hum Mol Genet 2009; 19:420-33; PMID:19884170; http://dx.doi.org/10.1093/hmg/ddp506
41. Balabanian S, Gendron NH, MacKenzie AE. Histologic and transcriptional assessment of a mild SMA model. Neurol Res 2007; 29:413-24; PMID:17535551; http://dx.doi.org/10.1179/016164107X159243
42. Lotti F, Imlach Wendy L, Saieva L, Beck Erin S, Hao Le T, Li Darrick K, Jiao W, Mentis GZ, Beattie CE, McCabe BD, et al. An SMN-dependent U12 splicing event essential for motor circuit function. Cell 2012; 151:440-54; PMID:23063131; http://dx.doi.org/10.1016/j.cell.2012.09.012
43. Zhang Z, Pinto AM, Wan L, Wang W, Berg MG, Oliva I, et al. Dysregulation of synaptogenesis genes antecedes motor neuron pathology in spinal muscular atrophy. Proc Nat Acad Sci 2013; PMID:24191055; 10.1073/pnas.1319280110
44. Meyer K, Marquis J, Trüb J, Nlend Nlend R, Verp S, Ruepp MD, Imboden H, Barde I, Trono D, Schümperli D., et al. Rescue of a severe mouse model for spinal muscular atrophy by U7 snRNA-mediated splicing modulation. Hum Mol Genet 2009; 18:546-55; PMID:19010792; http://dx.doi.org/10.1093/hmg/ddn382
45. Monani UR, Sendtner M, Coovert DD, Parsons DW, Andreassi C, Le TT, Jablonka S, Schrank B, Rossoll W, Prior TW, et al. The human centromeric survival motor neuron gene (SMN2) rescues embryonic lethality in smn(-/-) mice and results in a mouse with spinal muscular atrophy. Hum Mol Genet 2000; 9:333-9; PMID:10655541; http://dx.doi.org/10.1093/hmg/9.3.333
46. Voigt T, Meyer K, Baum O, Schümperli D. Ultrastructural changes in diaphragm neuromuscular junctions in a severe mouse model for spinal muscular atrophy and their prevention by bifunctional U7 snRNA correcting SMN2 splicing. Neuromuscul Disord 2010; 20:744-52; PMID:20832308; http://dx.doi.org/10.1016/j.nmd.2010.06.010
47. Voigt T, Neve A, Schümperli D. The craniosacral progression of muscle development influences the emergence of neuromuscular junction alterations in a severe murine model for spinal muscular atrophy. Neuropathol Appl Neurobiol 2014; 40:416-34; PMID:23718187; http://dx.doi.org/10.1111/nan.12064
48. Konig J, Zarnack K, Rot G, Curk T, Kayikci M, Zupan B, Turner DJ, Luscombe NM, Ule J. iCLIP reveals the function of hnRNP particles in splicing at individual nucleotide resolution. Nat Struct Mol Biol 2010; 17:909-15; PMID:20601959; http://dx.doi.org/10.1038/nsmb.1838
49. Cartwright P, Muller H, Wagener C, Holm K, Helin K. E2F-6: a novel member of the E2F family is an inhibitor of E2F-dependent transcription. Oncogene 1998; 17:611-23; PMID:9704927; http://dx.doi.org/10.1038/sj.onc.1201975
50. Hirst J, Borner GH, Harbour M, Robinson MS. The aftiphilin/p200/gamma-synergin complex. Mol Biol Cell 2005; 16:2554-65; PMID:15758025; http://dx.doi.org/10.1091/mbc.E04-12-1077
51. Burman JL, Wasiak S, Ritter B, de Heuvel E, McPherson PS, Hirst J, et al. Aftiphilin is a component of the clathrin machinery in neurons: the aftiphilin/p200/gamma-synergin complex. FEBS Letters 2005; 579:2177-84; PMID:15811338; http://dx.doi.org/10.1016/j.febslet.2005.03.008
52. Fujiwara I, Remmert K, Hammer JA. Direct observation of the uncapping of capping protein-capped actin filaments by CARMIL homology domain 3. J Biol Chem 2010; 285:2707-20; PMID:19926785; http://dx.doi.org/10.1074/jbc.M109.031203
53. Hernandez-Valladares M, Kim T, Kannan B, Tung A, Aguda AH, Larsson M, Cooper JA, Robinson RC. Structural characterization of a capping protein interaction motif defines a family of actin filament regulators. Nat Struct Mol Biol 2010; 17:497-503; PMID:20357771; http://dx.doi.org/10.1038/nsmb.1792
54. Yang C, Pring M, Wear MA, Huang M, Cooper JA, Svitkina TM, Zigmond SH. Mammalian CARMIL inhibits actin filament capping by capping protein. Dev Cell 2005; 9:209-21; PMID:16054028; http://dx.doi.org/10.1016/j.devcel.2005.06.008
55. Liang Y, Cucchetti M, Roncagalli R, Yokosuka T, Malzac A, Bertosio E, Imbert J, Nijman IJ, Suchanek M, Saito T, et al. The lymphoid lineage-specific actin-uncapping protein rltpr is essential for costimulation via CD28 and the development of regulatory T cells. Nat Immunol 2013; 14:858-66; PMID:23793062; http://dx.doi.org/10.1038/ni.2634
56. Shibata H, Huynh DP, Pulst S-M. A novel protein with RNA-binding motifs interacts with ataxin-2. Hum Mol Genet 2000; 9:1303-13; PMID:10814712; http://dx.doi.org/10.1093/hmg/9.9.1303
57. Kinoshita M, Noda M. Roles of septins in the mammalian cytokinesis machinery. Cell Struct Funct 2001; 26:667-70; PMID:11942624; http://dx.doi.org/10.1247/csf.26.667
58. Leshinsky-Silver E, Ginzberg M, Dabby R, Sadeh M, Lev D, Lerman-Sagie T. Neonatal vocal cord paralysis-an early presentation of hereditary neuralgic amyotrophy due to a mutation in the SEPT9 gene. Europ J Paediat Neurol 2013; 17:64-7; PMID:22981636; http://dx.doi.org/10.1016/j.ejpn.2012.08.006
59. Ahmad S, Wang Y, Shaik GM, Burghes AH, Gangwani L. The zinc finger protein ZPR1 is a potential modifier of spinal muscular atrophy. Hum Mol Genet 2012; 21:2745-58; PMID:22422766; http://dx.doi.org/10.1093/hmg/dds102
60. Chen IT, Chasin LA. Direct selection for mutations affecting specific splice sites in a hamster dihydrofolate reductase minigene. MolCell Biol 1993; 13:289-300; PMID:8417332
61. Black DL. Mechanisms of alternative pre-messenger RNA splicing. Annu Rev Biochem 2003; 72:291-336; PMID:12626338; http://dx.doi.org/10.1146/annurev.biochem.72.121801.161720
62. De Conti L, Baralle M, Buratti E. Exon and intron definition in pre-mRNA splicing. Wiley Interdiscipl Rev RNA 2013; 4:49-60; PMID:23044818; http://dx.doi.org/10.1002/wrna.1140
63. Kawahara Y, Ito K, Sun H, Aizawa H, Kanazawa I, Kwak S. Glutamate receptors: RNA editing and death of motor neurons. Nature 2004; 427:801-; PMID:14985749; http://dx.doi.org/10.1038/427801a
64. Kwak S, Kawahara Y. Deficient RNA editing of GluR2 and neuronal death in amyotropic lateral sclerosis. J Mol Med 2005; 83:110-20; PMID:15624111; http://dx.doi.org/10.1007/s00109-004-0599-z
65. Liu H, Shafey D, Moores JN, Kothary R. Neurodevelopmental consequences of Smn depletion in a mouse model of spinal muscular atrophy. J Neurosci Res 2010; 88:111-22; PMID:19642194; http://dx.doi.org/10.1002/jnr.22189
66. Leeb M, Pasini D, Novatchkova M, Jaritz M, Helin K, Wutz A. Polycomb complexes act redundantly to repress genomic repeats and genes. Genes Dev 2010; 24:265-76; PMID:20123906; http://dx.doi.org/10.1101/gad.544410
67. Dluzniewska J, Sarnowska A, Beresewicz M, Johnson I, Srai SK, Ramesh B, Goldspink G, Górecki DC, Zabłocka B. et al. A strong neuroprotective effect of the

autonomous C-terminal peptide of IGF-1 $_{Ec}$ (MGF) in brain ischemia. FASEB J 2005; 19:1896-8; PMID:16144956

68. Dobrowolny G, Giacinti C, Pelosi L, Nicoletti C, Winn N, Barberi L, Molinaro M, Rosenthal N, Musarò A. Muscle expression of a local igf-1 isoform protects motor neurons in an ALS mouse model. J Cell Biol 2005; 168:193-9; PMID:15657392; http://dx.doi.org/10.1083/jcb.200407021
69. Imlach WL, Beck ES, Choi BJ, Lotti F, Pellizzoni L, McCabe BD. SMN is required for sensory-motor circuit function in drosophila. Cell 2012; 151:427-39; PMID:23063130; http://dx.doi.org/10.1016/j.cell.2012.09.011
70. Singh NN, Singh RN. Alternative splicing in spinal muscular atrophy underscores the role of an intron definition model. RNA Biol 2011; 8:600-6; PMID:21654213; http://dx.doi.org/10.4161/rna.8.4.16224
71. Singh NN, Seo J, Ottesen EW, Shishimorova M, Bhattacharya D, Singh RN. TIA1 Prevents skipping of a critical exon associated with spinal muscular atrophy. Mol Cell Biol 2011; 31:935-54; PMID:21189287; http://dx.doi.org/10.1128/MCB.00945-10
72. Duncan PI, Stojdl DF, Marius RM, Scheit KH, Bell JC. The clk2 and clk3 dual-specificity protein kinases regulate the intranuclear distribution of SR proteins and influence pre-mRNA splicing. Exp Cell Res 1998; 241:300-8; PMID:9637771; http://dx.doi.org/10.1006/excr.1998.4083
73. Paillusson A, Hirschi N, Vallan C, Azzalin CM, Mühlemann O. A GFP-based reporter system to monitor nonsense-mediated mRNA decay. Nucleic Acids Res 2005; 33:e54; PMID:15800205; http://dx.doi.org/10.1093/nar/gni052
74. Ruepp MD, Vivarelli S, Pillai R, Kleinschmidt N, Azzouz TN, Barabino SM, Schümperli D. The 68 kDa subunit of mammalian cleavage factor I interacts with the U7 small nuclear ribonucleoprotein and participates in 3' end processing of animal histone mRNAs. Nucleic Acids Res 2010; 38:7637-50; PMID:20634199; http://dx.doi.org/10.1093/nar/gkq613
75. Marquis J, Kämpfer SS, Angehrn L, Schümperli D. Doxycycline-controlled splicing modulation by regulated antisense U7 snRNA expression cassettes. Gene Ther 2009; 16:70-7; PMID:18701908; http://dx.doi.org/10.1038/gt.2008.138
76. Bustin SA, Benes V, Garson JA, Hellemans J, Huggett J, Kubista M, Mueller R, Nolan T, Pfaffl MW, Shipley GL, et al. The MIQE guidelines: minimum information for publication of quantitative real-time PCR experiments. Clin Chem 2009; 55:611-22; PMID:19246619; http://dx.doi.org/10.1373/clinchem.2008.112797
77. Galiveti CR, Rozhdestvensky TS, Brosius J, Lehrach H, Konthur Z. Application of housekeeping npcRNAs for quantitative expression analysis of human transcriptome by real-time PCR. RNA 2010; 16:450-61; PMID:20040593; http://dx.doi.org/10.1261/rna.1755810